Influence of Stoichiometry and Charge State on the Structure and Reactivity of Cobalt Oxide Clusters with CO

ARTICLE *in* THE JOURNAL OF PHYSICAL CHEMISTRY A · NOVEMBER 2008

Impact Factor: 2.69 · DOI: 10.1021/jp805186r · Source: PubMed

6 AUTHORS, INCLUDING:

Grant Johnson
Pacific Northwest National Laboratory
44 PUBLICATIONS **982** CITATIONS
SEE PROFILE

Jose Ulises Reveles
Virginia Commonwealth University
76 PUBLICATIONS **1,423** CITATIONS
SEE PROFILE

Influence of Stoichiometry and Charge State on the Structure and Reactivity of Cobalt Oxide Clusters with CO

Grant E. Johnson,[†] J. Ulises Reveles,[‡] Nelly M. Reilly,[†] Eric C. Tyo,[†] Shiv N. Khanna,[‡] and A. W. Castleman, Jr.[†,*]

Departments of Chemistry and Physics, The Pennsylvania State University, University Park, Pennsylvania 16802 and Department of Physics, Virginia Commonwealth University, Richmond, Virginia 23284-2000

Received: June 12, 2008; Revised Manuscript Received: August 26, 2008

Cationic and anionic cobalt oxide clusters, generated by laser vaporization, were studied using guided-ion-beam mass spectrometry to obtain insight into their structure and reactivity with carbon monoxide. Anionic clusters having the stoichiometries $Co_2O_3^-$, $Co_2O_5^-$, $Co_3O_5^-$ and $Co_3O_6^-$ were found to exhibit dominant products corresponding to the transfer of a single oxygen atom to CO, indicating the formation of CO_2. Cationic clusters, in contrast, displayed products resulting from the adsorption of CO onto the cluster accompanied by the loss of either molecular O_2 or cobalt oxide units. In addition, collision induced dissociation experiments were conducted with N_2 and inert xenon gas for the anionic clusters, and xenon gas for the cationic clusters. It was found that cationic clusters fragment preferentially through the loss of molecular O_2 whereas anionic clusters tend to lose both atomic oxygen and cobalt oxide units. To further analyze how stoichiometry and ionic charge state influence the structure of cobalt oxide clusters and their reactivity with CO, first principles theoretical electronic structure studies within the density functional theory framework were performed. The calculations show that the enhanced reactivity of specific anionic cobalt oxides with CO is due to their relatively low atomic oxygen dissociation energy which makes the oxidation of CO energetically favorable. For cationic cobalt oxide clusters, in contrast, the oxygen dissociation energies are calculated to be even lower than for the anionic species. However, in the cationic clusters, oxygen is calculated to bind preferentially in a less activated molecular O_2 form. Furthermore, the CO adsorption energy is calculated to be larger for cationic clusters than for anionic species. Therefore, the experimentally observed displacement of weakly bound O_2 units through the exothermic adsorption of CO onto positively charged cobalt oxides is energetically favorable. Our joint experimental and theoretical findings indicate that positively charged sites in bulk-phase cobalt oxides may serve to bind CO to the catalyst surface and specific negatively charged sites provide the activated oxygen which leads to the formation of CO_2. These results provide molecular level insight into how size, stoichiometry, and ionic charge state influence the oxidation of CO in the presence of cobalt oxides, an important reaction for environmental pollution abatement.

Introduction

Nanoscale clusters have been shown to exhibit large changes in their structural and electronic properties with the incorporation or removal of single atoms.[1] Consequently, in this size regime, in which each atom counts, it is possible to obtain substantial variations in chemical reactivity by adjusting the size and stoichiometry of small clusters. Previously, we comprehensively examined the reactivity of carbon monoxide (CO) with both anionic[2,4] and cationic[3,4] iron oxide clusters. We demonstrated, through a combination of experiment and theory, that clusters containing one more oxygen atom than iron atom are the most reactive anionic iron oxides for CO oxidation.[2] The enhanced reactivity of these anionic species was attributed to the relatively low dissociation energy of atomic oxygen which makes the oxidation of CO thermodynamically favorable, and to the ability of the clusters to structurally rearrange which lowers the reaction barriers.[2] Furthermore, a systematic study of cationic iron oxide clusters containing one and two iron atoms revealed that species with three or fewer oxygen atoms are the most selective species for CO oxidation whereas oxygen rich cationic clusters exhibit CO adsorption products and, consequently, a lower selectivity toward oxidation.[3] An analysis of the influence of ionic charge state on the oxidation of CO by $FeO_3^{\pm}$ was also conducted demonstrating that the positively charged cluster is far more reactive.[4] Based on these previous findings, it is reasonable to expect that specific oxide clusters of the other 3d transition metals may exhibit enhanced reactivity for the oxidation of simple molecules such as CO.

Cobalt oxide is widely employed as both a catalyst and catalyst support material in a variety of industrially relevant reactions. For example, recent studies have shown that cobalt oxide catalysts are highly active for the oxidation of CO at ambient temperatures[5,6] and the complete[7] as well as selective[8] oxidation of short chain alkanes such as propane. These studies provide insight into the preparation and reactive behavior of bulk-phase cobalt oxide catalysts. However, the nature of the active sites and the molecular-level mechanisms of the oxidation reactions remain to be determined.

Gas-phase cluster experiments allow catalyst materials, such as cobalt oxide, to be studied in the absence of factors which complicate condensed-phase research,[9] as discrepancies resulting from different preparation methods can exert a pronounced

* Corresponding author: Email: awc@psu.edu, Tel: (814)-865-7242, Fax: (814)-865-5235

[†] The Pennsylvania State University.

[‡] Virginia Commonwealth University.

10.1021/jp805186r CCC: $40.75
Published on Web 10/15/2008

influence on catalytic activity. Gas-phase studies avoid these inconsistencies and allow for the physical and chemical behavior of catalyst materials to be studied with atomic level precision.[10] Previous studies, employing photoelectron spectroscopy (PES) investigated the evolution of the electronic structure of $Co_xO_y^-$ ($x = 4-20$, $y = 0-2$) clusters.[11] For the smaller clusters an increase in electron affinity (EA) was observed with increasing oxygen saturation.[11] Furthermore, the $Co_4O_3^-$ and $Co_5O_3^-$ clusters were determined to have geometric isomers with both peroxo and ozonide structures.[11] These findings were supported by theoretical calculations which revealed that CoO_y ($y = 3-4$) neutral clusters with peroxide structures are more stable than the alternative oxide isomers.[12] Clusters with peroxide units should exhibit enhanced oxidation reactivity because the peroxide bond is formally a O−O single bond in comparison to the O═O double bond in molecularly adsorbed oxygen. Indeed, the activation of the strong O═O bond has been proposed to be the rate limiting step for the oxidation of CO in the presence of gold clusters.[13] Other gas-phase studies of the reactivity of cationic cobalt clusters[14] with O_2 revealed higher rate constants for the cations than for the corresponding neutral[15] and anionic species.[16] These previous findings raise fundamental questions as to how stoichiometry and ionic charge state may influence the structure and reactivity of cobalt oxide clusters.

In the present study, we demonstrate that specific anionic cobalt oxide clusters are particularly reactive toward the oxidation of CO to CO_2. Theoretical calculations indicate that the enhanced reactivity of these anionic clusters is due to their relatively low atomic oxygen dissociation energy which makes the oxidation reaction energetically favorable. Cationic clusters, in contrast, are found to react preferentially through the adsorption of CO accompanied by the loss of either molecular O_2 or cobalt oxide units. Calculations show that the oxygen dissociation energy for cationic cobalt oxide clusters is significantly lower than for the anionic species. Consequently, oxygen in the cationic clusters binds in a less activated molecular O_2 form. In addition, the CO binding energy for cationic clusters is calculated to be much larger than for anionic cobalt oxides. Therefore, the experimentally observed displacement of weakly bound O_2 molecules through the exothermic adsorption of CO onto positively charged clusters is energetically favorable. Collision induced dissociation experiments reveal that anionic clusters fragment mainly through the loss of atomic oxygen or cobalt oxide units whereas cationic clusters favor the loss of molecular O_2. Anionic cobalt oxide clusters, therefore, contain a larger proportion of atomically bound oxygen than cationic species. The bonding motifs suggested by the fragmentation products agree well with the theoretically calculated structures. Our findings provide molecular level insight into how ionic charge state and stoichiometry influence the structure and reactivity of cobalt oxide clusters with CO.

Experimental Methods

The reactivity of anionic and cationic cobalt oxide clusters with CO was studied using a guided-ion-beam mass spectrometer described in detail in a previous publication.[17] Briefly, ionic cobalt oxide clusters were produced in a laser vaporization (LaVa) cluster source by pulsing oxygen seeded in helium (10%) into the plasma formed by ablating a cobalt rod with the second harmonic (532 nm) of a Nd:YAG laser. The clusters exit the source region through a 27 mm long conical expansion nozzle and are cooled through supersonic expansion into vacuum. During supersonic expansion the high pressure (13.2 atm) expansion gas mixture passes through a narrow diameter nozzle into vacuum. The random thermal energy of the clusters is thereby converted into directed kinetic energy of the molecular beam. Consequently, the internal vibrational and rotational energy of the clusters is lowered through collisions with the He carrier gas. The kinetic energy imparted to the cluster ions by the supersonic expansion was determined, employing a retarding potential analysis,[17] to be approximately 1 eV in the laboratory energy frame (E_{LAB}). Ideally, all clusters exiting the supersonic expansion source have the same initial kinetic energy. Using eq 1

$$E_{CM} = E_{LAB}\frac{\text{Mass[CO]}}{\text{Mass[cluster]} + \text{Mass[CO]}} \quad (1)$$

the initial center-of-mass collision energy (E_{CM}) was calculated for $CoO_2^{\pm}$, $Co_2O_4^{\pm}$, and $Co_3O_5^{\pm}$ to be approximately 0.24, 0.13, and 0.09 eV with CO, respectively. As subsequent collisions are expected to dissipate the initial energy of a given cluster the values reported above serve to establish an upper limit on the kinetic energy of the reactive collisions.

After exiting the source region, the clusters pass through a 3 mm skimmer forming a collimated molecular beam and are directed into a quadrupole mass filter employing a set of electrostatic lenses. The quadrupole mass filter isolates clusters of a desired mass that are then passed into an octopole collision cell. Variable pressures of CO, N_2 or Xe are introduced into the octopole collision cell employing a low flow leak valve. The gas pressure is monitored using a MKS Baratron capacitance manometer. Product ions formed in the collision cell are mass analyzed by a second quadrupole mass spectrometer. Finally, the ions are detected with a channeltron electron multiplier connected to a mutichannel scalar card. The experimental branching ratios presented in the results section illustrate the change in normalized ion intensity with increasing pressures of CO reactant gas. At higher gas pressures the ratio of reactant ion intensity to total ion intensity becomes smaller whereas the ratio of product ion intensity to total ion intensity becomes larger. Control experiments were also conducted with N_2 to verify that the products observed with CO are the result of a chemical reaction and not the products of collisional fragmentation, given that both CO and N_2 are of the same nominal mass. In addition, collision induced dissociation studies were performed using inert Xe gas at three pressures, 0.08, 0.12, and 0.22 mTorr. During these experiments the kinetic energy of the cluster ions is increased by applying an accelerating DC potential of between 0 and 40 V to the octopole rods. The fragmentation products, therefore, are observed according to the collision energy required to generate them and hence aid in identifying the structural properties of the clusters. The overall chemical and collisional processes observed experimentally are presented as equations in the section of results.

Theoretical Methods

First principles electronic structure studies were performed within the generalized gradient density functional theory (DFT) formalism. The actual calculations were carried out using the linear combination of Gaussian type orbitals DFT Kohn−Sham approach as implemented in the deMon2k[18] code. The exchange and correlation effects were incorporated through the PW86 generalized gradient approximation (GGA) functional proposed by Perdew et al.[19] Further, the double-ζ with valence polarization (DZVP) basis sets optimized for gradient corrected exchange−correlation functionals were used.[20] More details about the numerical procedure can be found in previous publications.[2−4] For each cluster structure and charge state, the configuration

space was sampled and optimized by starting from several initial configurations and spin multiplicities. A vibrational analysis was performed to distinguish between minima and transition states. Our studies revealed close spaced local minima on the potential energy surfaces of neutral and charged Co_xO_y clusters as reported in a previous DFT study of CoO_y ($y = 1-4$) neutral and anionic clusters.[12]

To further eliminate any uncertainty associated with the choice of basis set or the numerical procedure, we carried out supplementary calculations using the Naval Research Laboratory Molecular Orbital Library (NRLMOL) set of codes developed by Pederson and co-workers.[21−23] For these calculations the PW91 generalized gradient approximation[24] was employed. A 5s, 4p and 3d basis set for the C and O atoms and 7s, 5p and 4d basis set for the Co atom was used.[23] In each case, the basis set was supplemented by a diffuse Gaussian. We found very good agreement between the deMon2k and NRLMOL calculations. In general both methods predicted the same ground state multiplicities and geometries with differences in the range of 1 to 6 pm in the bond lengths. The deMon2k calculations were found to consistently predict longer Co−Co bonds when compared with the NRLMOL calculations with the largest deviations for the Co_2 neutral and charged clusters. Even though no experimental bond length is available for the Co_2 dimer, empirical estimations of 2.02 ± 0.35 and 2.31 Å have been reported by Weisshaar[25] and Kant et al.,[26] respectively. On the other hand, a bond length around 2 Å has been reported in most theoretical works,[27−31] whereas longer bond lengths between 2.20 and 2.56 Å have been reported in recent configuration interaction[32] and DFT reports.[20,33] In our case, the NRLMOL calculations predicted a dimer bond length of 1.99 Å in agreement with most previous DFT works. Beyond the good agreement between the deMon2k and NRLMOL calculations, NRLMOL allowed us to investigate antiferromagnetic configurations for the clusters with two Co atoms, and these states were found to be the actual ground states for some clusters. For this reason we only report here the results based on the NRLMOL calculations. All the molecular geometries were plotted with the Schakal software.[34]

The benchmarks on the accuracy of the theoretical calculations on oxide clusters were established via calculations of the bond lengths, dissociation energies (DE), ionization potentials (IP), and electron affinities (EA) of O_y, CO_y ($y = 1, 2$) and neutral and cationic Co_xO_y ($x = 1-2$; $y = 1-2$) clusters, and their comparison with the available corresponding experimental values.[25,26,35−47] These results are collected in Table 1. We found that the bond lengths are in good agreement with experiments, DE's are higher than the experimental dissociation energies, and the calculated IP's and EA's presented good agreement with respect to the experimental values. Higher DE's are known to occur generally in density functional theory.[48] Additionally, in general we found good agreement in the ground state spin configurations and geometries of the neutral and anionic CoO_y ($y = 1-4$) clusters, with respect to a previous theoretical study,[12] as described in the Results and Discussion. Finally, we found an increase in the electron affinity with increasing oxygen saturation in agreement with experimental studies of $Co_xO_y^-$ ($x = 4-20$, $y = 0-2$) clusters.[11] Although our calculations overestimate the energies, it is important to highlight that the discussion is based on relative differences in the dissociation and binding energies, and we are confident about the conclusions based on the current approach.

TABLE 1: Comparison of Calculated Bond Lengths in Å, Dissociation Energies (DE), Ionization Potentials (IP) and Electron Affinities (EA) of O, O_2, CO, CO_2 and Co_xO_y ($x = 1, 2$; $y = 0-2$) Clusters with Respect to Experimental Studies[a]

	bond (exp)	bond (this work)	DE (exp)	DE (this work)
$^3O_2$	1.21[35]	1.22	5.17 (0.002)[36]	6.18
^1CO	1.13[37]	1.14	11.156 (0.007)[36]	11.62
$^1CO_2$ (OC−O)	1.16[38]	1.17	5.54[39]	6.34
$^5Co_2$	2.02 (0.35)[b,25] 2.31[b,26]	1.99	≤1.32[40] 1.72[26]	2.51
$^6Co_2^+$		2.09	2.765 (0.001)[41]	3.27
^4CoO	1.63[c,12]	1.63	3.98 (0.14)[36]	4.97
$^5Co^+$−O		1.63	3.29 (0.05)[36]	4.13
$^6Co_2^+$−O		1.72	4.46 (0.15)[42]	5.28

	IP (exp)	IP (this work)	EA (exp)	EA (this work)
^3O	13.619[37]	14.11	1.4611[43]	1.64
$^3O_2$	12.071[37]	12.42	0.45 (0.002)[43]	0.36
^4Co	7.88[44]	7.92	0.662 (0.003)[43]	0.84
$^5Co_2$	≤6.42[40]	7.16	1.11 (0.008)[43]	0.72
^4CoO	8.57 (0.15)[45] 8.71 (0.20)[40] 9.0 (0.05)[41]	8.76	1.45[46]	1.30
$^2CoO_2$		10.05	2.97[47]	2.78

[a] Uncertainty is given in parentheses. The superscripts indicate spin multiplicity. All energy values are given in units of eV. [b] Empirical estimations. [c] Theoretical study.

Results and Discussion

Reactivity Studies. A systematic study of both cationic and anionic cobalt oxide clusters was undertaken to determine the influence of size, stoichiometry, and ionic charge state on structure and reactivity. Typical mass distributions of anionic and cationic cobalt oxide clusters obtained through laser vaporization are displayed in Figure 1a,b, respectively. Anionic clusters containing between one and three cobalt atoms and two to six oxygen atoms were reacted with CO. Cationic clusters with one and two cobalt atoms and between one and six oxygen atoms were also investigated. Table 2 summarizes the products observed from the interaction of these cobalt oxide clusters with CO, N_2 or Xe. Clusters that exhibit dominant atomic oxygen transfer products with CO but not with N_2 or Xe are proposed to be reactive for the oxidation of CO to CO_2. Clusters that lose atomic oxygen with N_2 are considered to be unreactive as the products result from collisional fragmentation and not chemical reaction.

Inspection of Table 2 reveals that the anionic cobalt oxides $Co_2O_3^-$, $Co_2O_5^-$, $Co_3O_5^-$ and $Co_3O_6^-$ exhibit dominant atomic oxygen transfer products when reacted with CO suggesting that they are active for the oxidation of CO to CO_2. The normalized ion intensities of these clusters with increasing pressures of CO reactant gas are displayed in Figure 2. The reactant ions $Co_2O_3^-$, $Co_2O_5^-$, $Co_3O_5^-$ and $Co_3O_6^-$ decrease in normalized intensity with increasing pressure of CO whereas the respective dominant product ions, $Co_2O_2^-$, $Co_2O_4^-$, $Co_3O_4^-$, and $Co_3O_5^-$ become more pronounced. These products result from the transfer of a single oxygen atom to CO forming CO_2 according to eq 2.

$$Co_xO_y^- + CO \rightarrow Co_xO_{y-1}^- + CO_2 \quad (2)$$

As shown in Figure 2a, the $Co_2O_3^-$ cluster also exhibits a minor CoO_2^- product which forms according to eq 3.

$$Co_2O_3^- + CO \rightarrow CoO_2^- + Co + CO_2 \quad (3)$$

CoO_2^- was not observed in separate experiments with N_2 indicating that it results from the exothermic oxidation of CO

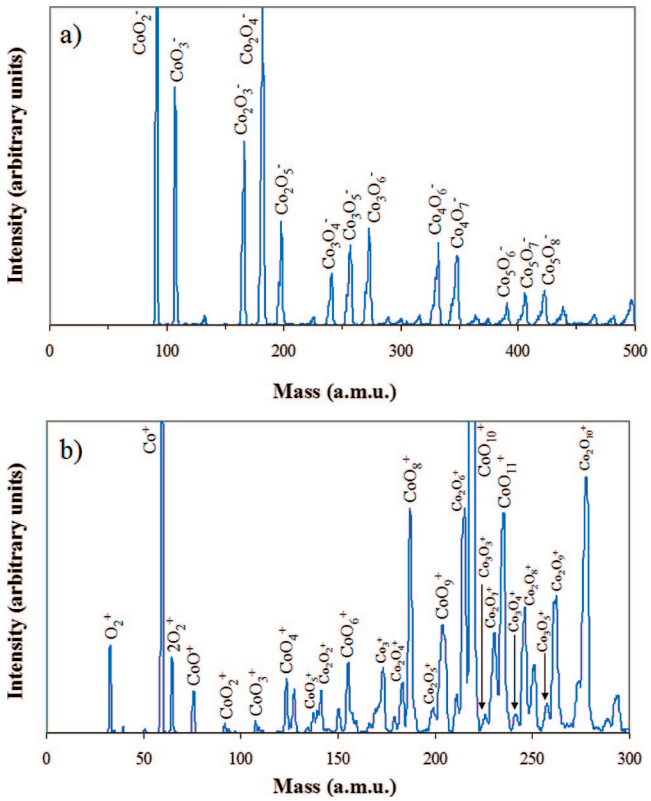

Figure 1. Typical mass distribution of (a) anionic and (b) cationic cobalt oxide clusters obtained through laser vaporization.

by $Co_2O_3^-$. Indeed, in fragmentation studies of $Co_2O_3^-$ with Xe at higher collision energies, CoO_2^- is observed. Therefore, a considerable amount of energy is required, in the form of either kinetic energy or chemical heat of formation, to generate CoO_2^- from $Co_2O_3^-$. In addition, it is reasonable that the more oxygen rich CoO_2^- fragment retains the additional electron of the anion, as according to our calculations CoO_2 has a higher electron affinity of 2.78 eV compared to only 0.84 eV for Co. The calculated electron affinities and ionization potentials of the cobalt oxide clusters are provided in Tables 3 and 4. The minor products for the $Co_2O_5^-$ cluster, displayed in Figure 2b, result from the collisional loss of O_2 and CoO_2 forming $Co_2O_3^-$ and CoO_3^-, respectively, according to eqs 4 and 5.

$$Co_2O_5^- + CO \rightarrow Co_2O_3^- + O_2 + CO \quad (4)$$

$$Co_2O_5^- + CO \rightarrow CoO_3^- + CoO_2 + CO \quad (5)$$

Both of these products were observed in separate experiments with N_2 confirming that they result from collisional fragmentation of $Co_2O_5^-$. In eq 5, it is reasonable that the CoO_3^- fragment retains the additional electron of the anion as it has a higher calculated electron affinity of 3.97 eV whereas that of CoO_2 is 2.78 eV. For $Co_2O_5^-$ a minor atomic oxygen loss product was observed with N_2 but was of much lower intensity than with CO. The larger three cobalt atom clusters also exhibited minor products as shown in Figure 2c,d. Specifically, the $Co_3O_5^-$ cluster loses two oxygen atoms forming $Co_3O_3^-$ according to eq 6.

$$Co_3O_5^- + 2CO \rightarrow Co_3O_3^- + 2CO_2 \quad (6)$$

O_2 loss from $Co_3O_5^-$ was not observed in separate experiments with N_2, indicating that $Co_3O_3^-$ results from the exothermic oxidation of two CO molecules. $Co_3O_6^-$ loses molecular O_2, atomic oxygen and molecular O_2, and atomic oxygen and CoO

TABLE 2: List of Products Co_xO_y (*x*,*y*) Resulting from the Chemical Reactions between Mass Selected Cobalt Oxide Clusters and Carbon Monoxide[a]

Cobalt Oxide Anions

$Co_xO_y^-$ (*x*,*y*)	products with CO	products with N_2	products with Xe	neutral(s) lost with Xe
1,2	1,1	none	1,1	0,1
1,3	1,2	1,2	1,2	0,1
2,3	2,2	2,1	1,2	1,1
	1,2		2,2	0,1
2,4	2,3[c]	none	1,3	1,1
			1,2	1,2
			2,3	0,1
2,5	2,4	2,4	2,3	0,2
	2,3	2,3	1,3	1,2
	1,3	1,3	2,4	0,1
			1,2	1,3
3,4	3,3[c]	none		
	2,4[c]			
3,5	3,4	none	3,3	0,2
	3,3		3,4	0,1
	2,3[c]		2,4	
	2,4[c]		2,3	
3,6	3,5	3,4	3,4	0,2[b]
	3,4	3,5	3,5	0,1
	3,3		2,4	1,2
	2,4		3,3	0,3
	2,3		2,3	1,3

Cobalt Oxide Cations

$Co_xO_y^+$ (*x*,*y*)	products with CO	products with Xe	neutral(s) lost with Xe
1,1	Co^+	1,0	0,1
1,2	$CoCO^+$	1,0	0,2
	Co^+	1,1	0,1
	$CoO(CO)_2^+$[c]		
1,3	$CoOCO^+$	1,1	0,2
	CoO^+	1,2	0,1
	Co^+		
	$CoO(CO)_2^+$ [c]		
1,4	CoO_2CO^+	1,2	0,2[b]
	$Co(CO)_2^+$	1,3	0,1[b]
	CoO_2^+		
	$CoCO^+$		
2,2	$Co(CO)_2^+$	2,1	0,1
	CoO_2CO^+	2,0	0,2
2,4	$Co_2O_2^+$	2,2	0,2[b]
	Co_2CO^+	2,0	0,4
	$Co(CO)_2^+$		
	CoO_2CO^+		
2,6	$Co_2O_4^+$	2,4	
	$Co_2O_2^+$	2,2	0,4[b]
	$Co(CO)_2^+$	2,1	0,5[b]
	$CoCO^+$ [c]	1,4	1,2
		1,2	1,4

[a] For the cationic clusters, the second column of the table lists the products as chemical formula rather than in the shorthand (*x*,*y*) notation due to the presence of CO association. Fragmentation products Co_xO_y (*x*,*y*) resulting from collision induced dissociation with inert N_2 and Xe are also shown for comparison. [b] Represents that dissociation occurs at near thermal energies. [c] Denotes a minor product channel whose relative intensity is less than 1% and not shown in the branching ratios for clarity.

to form $Co_3O_4^-$, $Co_3O_3^-$ and $Co_2O_4^-$, respectively, according to eqs 7a−7c.

$$Co_3O_6^- + CO \rightarrow Co_3O_4^- + O_2 + CO \quad (7a)$$

$$Co_3O_6^- + CO \rightarrow Co_3O_3^- + O_2 + CO_2 \quad (7b)$$

$$Co_3O_6^- + CO \rightarrow Co_2O_4^- + CoO + CO_2 \quad (7c)$$

Only minor loss of atomic and molecular oxygen from $Co_3O_6^-$

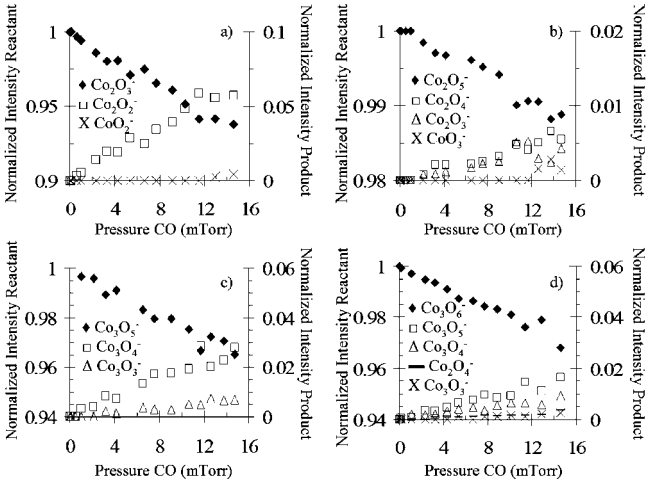

Figure 2. Normalized ion intensities of (a) $Co_2O_3^-$, (b) $Co_2O_5^-$, (c) $Co_3O_5^-$, and (d) $Co_3O_6^-$ and reaction products with increasing pressure of CO. Notice the decrease in the reactant ion intensity and the concomitant increase in the O-atom transfer products. The reactant ion intensity is plotted on the left *y* axis and the product on the right.

TABLE 3: Calculated Dissociation Energies of Atomic DE(O), and Molecular Oxygen DE(O_2) from Anionic, Neutral and Cationic CoO_y ($y = 1-4$) Clusters Corresponding to the Graphs in Figure 6[a]

	DE(O)	DE(O_2)	EA	IP
^4Co			0.84	7.92
^4CoO	4.97		1.30	8.76
$^2CoO_2$	4.76	3.55	2.78	10.05
$^2CoO_3$	4.07	2.66	3.97	10.37
$^4CoO_4$	3.39	1.29	3.06	9.82
$^5CoO^+$	4.13			
$^3CoO_2^+$	3.47	1.42		
$^3CoO_3^+$	3.75	1.05		
$^3CoO_4^+$	3.94	1.52		
$^5CoO^-$	5.43			
$^1CoO_2^-$	6.25	5.5		
$^3CoO_3^-$	5.26	5.33		
$^3CoO_4^-$	2.49	1.57		

[a] Electron affinities (EA), and ionization potentials (IP) of neutral CoO_y ($y = 0-4$) clusters. All values are given in units of eV.

was observed with N_2, again showing that the intensity of these products is greatly enhanced through the exothermic oxidation of CO. It should be noted that all of the minor products are lower in intensity than the atomic oxygen transfer products, indicating that these anionic cobalt oxide clusters are reasonably selective toward the oxidation of CO. The anionic cobalt oxide clusters that were not determined to be particularly reactive for the oxidation of CO exhibited either atomic or molecular oxygen loss in collisional studies with N_2 or Xe. A complete list of products is provided in Table 2. Both CoO_2^- and CoO_3^- showed small atomic oxygen loss products that accounted for approximately 1.5% of the total ion intensity at 15 mTorr of CO. On the basis of the results of fragmentation studies with N_2 and Xe, however, we believe that the atomic oxygen loss channel is collisional for CoO_3^-. The CoO_2^- cluster, in contrast, transfers an oxygen atom to CO and calculations indicate that the formation of CO_2 is slightly exothermic as discussed later in the section of theoretical results. Finally, very small atomic oxygen transfer products were observed for the reactions of $Co_2O_4^-$ and $Co_3O_4^-$ with CO. However, due to their negligible intensity we do not specify $Co_2O_4^-$ and $Co_3O_4^-$ as efficient oxidizers of CO.

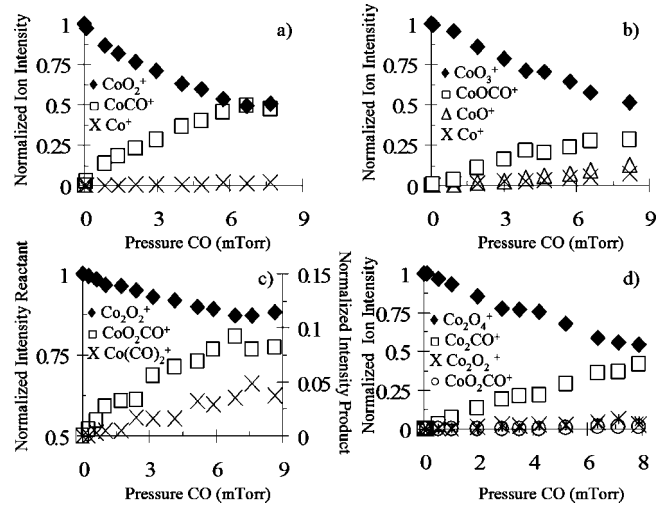

Figure 3. Normalized ion intensities of (a) CoO_2^+, (b) CoO_3^+, (c) $Co_2O_2^+$, and (d) $Co_2O_4^+$ and reaction products with increasing pressure of CO. Notice the decrease in the reactant ion intensity and the concomitant increase in the products corresponding to the adsorption of CO accompanied by the loss of O_2 or CoO_y. The normalized ion intensity is plotted on the left *y* axis.

Inspection of Table 2 reveals that the cationic cobalt oxide clusters react differently with CO compared to the anionic clusters. For cationic cobalt oxides containing one cobalt atom the dominant products correspond to the adsorption of one CO molecule onto the cluster accompanied by the loss of molecular O_2 according to eq 8.

$$CoO_y^+ + CO \rightarrow CoO_{y-2}^+ + CO + O_2 \quad (8)$$

This reaction is apparent from the normalized ion intensities of CoO_2^+ and CoO_3^+ with increasing CO pressure displayed in Figures 3a,b, respectively. For CoO_2^+, the dominant product, accounting for approximately 50% of the total ion intensity at 10 mTorr of CO, corresponds to the replacement of molecular O_2 by CO. Collisional studies with Xe also revealed molecular O_2 loss from CoO_2^+, indicating that O_2 is very weakly bound to the cobalt cation. A minor Co^+ product is also present in Figure 3a that may result from either collisional loss of O_2, as suggested by fragmentation experiments with Xe, or the oxidation of two CO molecules as indicated by theory in the next section. CoO_3^+ exhibits products corresponding to the replacement of O_2 by CO and, in addition, the collisional loss of O_2 as shown in Figure 3b. Again, fragmentation studies with Xe revealed loss of O_2 from CoO_3^+, albeit with lower intensity than with CO. A minor Co^+ product is also observed for the reaction of CoO_3^+ with CO. Collisional studies of CoO^+ with Xe revealed loss of atomic oxygen forming Co^+. For this reason we believe that the CoO^+ intermediate, which results from the loss of O_2 from CoO_3^+, undergoes further fragmentation according to eqs 9a and 9b.

$$CoO_3^+ + CO \rightarrow CoO^+ + O_2 + CO \quad (9a)$$

$$CoO^+ + CO \rightarrow Co^+ + O + CO \quad (9b)$$

However, we cannot exclude that CoO^+ may oxidize CO. Different products were observed for the cationic two cobalt atom clusters. As shown in Figure 3c, $Co_2O_2^+$ exhibits a dominant product resulting from the adsorption of CO accompanied by the loss of a Co atom according to eq 10.

$$Co_2O_2^+ + Co \rightarrow CoO_2(CO)^+ + Co \quad (10)$$

The loss of a cobalt atom from $Co_2O_2^+$ was not seen in

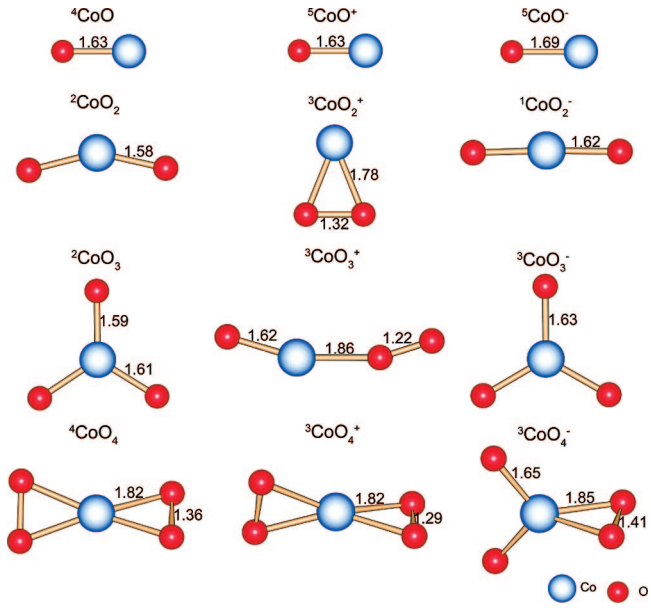

Figure 4. Calculated ground state geometries of neutral, cationic, and anionic CoO_y ($y = 1-4$) clusters. The bond lengths are given in angstroms and the superscripts indicate the spin multiplicity.

fragmentation studies with Xe, indicating that this product is not collisional but results from the exothermic adsorption of CO onto the cluster. The minor product for the reaction of $Co_2O_2^+$ with CO consists of a Co cation with two CO molecules attached $Co(CO)_2^+$ and results from the loss of CoO_2 according to eq 11.

$$Co_2O_2^+ + 2CO \rightarrow Co(CO)_2^+ + CoO_2 \qquad (11)$$

For the more oxygen rich $Co_2O_4^+$ cluster, the dominant product is $Co_2(CO)^+$, which results from the replacement of two O_2 molecules by one CO molecule according to eq 12.

$$Co_2O_4^+ + CO \rightarrow Co_2(CO)^+ + 2O_2 \qquad (12)$$

Loss of both one and two O_2 units from $Co_2O_4^+$ was observed in collisional studies with Xe confirming that these O_2 units are weakly bound and easily displaced through the exothermic adsorption of CO onto $Co_2O_4^+$. The minor products for the reaction of $Co_2O_4^+$ with CO, shown in Figure 3d, correspond to the replacement of O_2 by CO and the collisional loss of O_2. The remaining cationic cobalt oxide clusters displayed similar behavior to the example species discussed above and the products are listed in Table 2 for the sake of completeness.

Structural Analysis. To gain further insight into the influence of stoichiometry and charge state on the structure of cobalt oxide clusters and their reactivity with CO, first principles investigations within a density functional theory scheme were performed. The calculated ground state geometries for neutral, cationic and anionic cobalt oxide clusters containing one cobalt atom are shown in Figure 4. Although the experimental studies included only cationic and anionic clusters, we performed a theoretical study of the neutral species as well to enable a complete comparison of how charge state influences structure.

Neutral CoO_y ($y = 1-3$) clusters bind oxygen atomically to the Co atom with cobalt−oxygen bond lengths in the range 1.58−1.63 Å, whereas in CoO_4 the four oxygen atoms form two molecular O_2 units bonded to the Co atom at a larger cobalt−oxygen distance of 1.82 Å. The oxygen−oxygen bonds of the O_2 units in CoO_4 are elongated having bond lengths of 1.36 Å. The spin multiplicities are quartet for CoO and CoO_4 and doublet for CoO_2 and CoO_3. For the cationic CoO_y series with $y \geq 2$ the oxygen atoms form molecular O_2 units with oxygen−oxygen bond lengths in the range 1.22−1.32 Å, and bond to the Co atom at cobalt−oxygen bond lengths of 1.78−1.86 Å. The oxygen−oxygen bond is elongated in the O_2 units in CoO_2^+ and CoO_4^+ with lengths equal to 1.32 and 1.29 Å, respectively. The O−O bond length in the molecular O_2 unit in CoO_3^+ has a length of 1.22 Å, which is the same as an isolated O_2 molecule. The spin multiplicities are quintet for the CoO^+ cluster and triplet for the rest of the cationic series. In the case of the anionic CoO_y series, the optimized geometries resulted in structures similar to the neutral species with the oxygen atoms bonded atomically to the Co atom for $y \leq 3$. For the CoO_4^- cluster two oxygen atoms bind atomically to the Co atom and the other two form a molecular O_2 unit with an elongated O−O bond (1.41 Å).

In a B1LYP/CCSD(T) (CCSD(T) single point energy calculations of B1LYP optimized geometries) electronic structure study of CoO_y ($y = 1-4$), Uzunova et al. reported a large number of closed spaced minima and the existence of peroxide structures,[12] and in general our calculations agree well with this report. For CoO and CoO^- we predicted the same geometries and spin multiplicities. For the CoO_y ($y > 2$) neutral and anionic clusters our calculated geometries agreed with Uzunova et al., although higher multiplicities than the ones we found were reported to be the ground states. We further investigated this disagreement by performing additional calculations with the same methodology employed by Uzunova et al. in the Gaussian 03 package[49] and found that calculations with different functionals could invert the energetic ordering of the closed spaced minima. As an example, for CoO_3 Uzunova et al. reported, on the basis of B1LYP optimizations, that the ground state is an oxoperoxide in a sextet state, but an oxide in a doublet state was 1.47 eV higher in energy. This result is consistent with PBE[50] and B3LYP[51] optimizations using Gaussian 03, whereas PW91[24] predicted the oxide in a doublet state to be more stable, in agreement with our present study employing the PW91 functional and both the deMon2k and NRLMOL codes. Interestingly, though single point CCSD(T) calculations of the B1LYP optimized geometries predicted the sextet oxoperoxide to be the ground state, CCSD(T) single point calculations of the PBE, B3LYP and PW91 optimized structures predicted the oxide in a doublet state to be more stable than the sextet oxoperoxide. This indicates that the results based on CCSD(T) depend on the starting functional.

The calculations indicate that upon addition of a second oxygen atom to a single cobalt atom, significant structural differences become apparent between the different ionic charge states of cobalt oxide clusters. The CoO_2 neutral and anionic clusters both bind oxygen atomically. The neutral cluster is slightly bent, and the anion is linear. The CoO_2^+ cation, in comparison, contains a molecular O_2 unit with elongated cobalt−oxygen and oxygen−oxygen bonds. This structural variation with ionic charge state is confirmed by the experimental fragmentation data shown in Table 2 which indicates the loss of atomic oxygen from CoO_2^- and the loss of molecular oxygen from CoO_2^+. The CoO_3 neutral and anionic clusters bind oxygen exclusively in the atomic form. The cationic CoO_3^+, however, contains both an atomic and a molecular oxygen unit. The experimental fragmentation studies again confirm the results of the theoretical calculations showing that the anionic CoO_3^- loses atomic oxygen and the cation loses an intact O_2 molecule at low energy followed by atomic oxygen at higher energy. At a saturation of four oxygen atoms, both the neutral and cationic

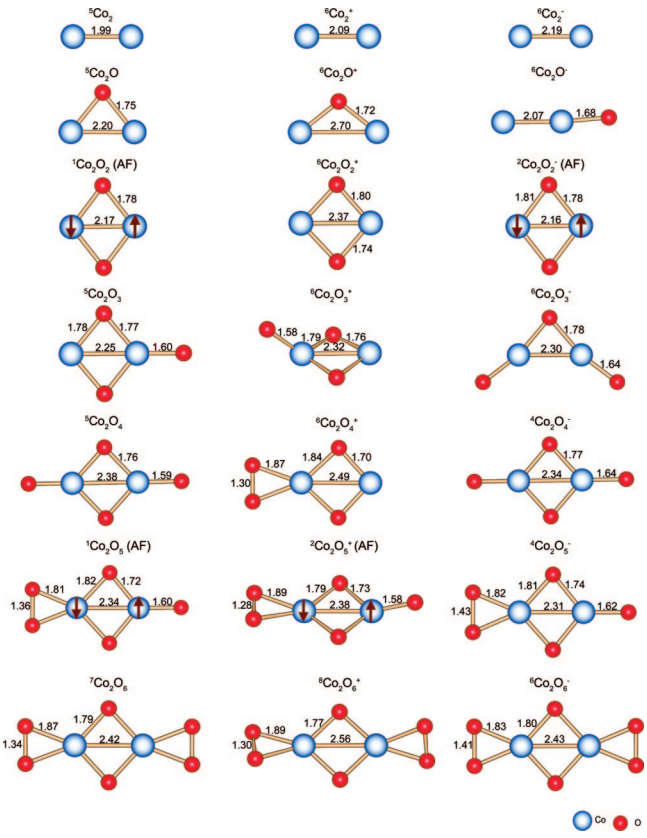

Figure 5. Calculated ground state geometries of neutral, cationic and anionic Co_2O_y ($y = 0-6$) clusters. The bond lengths are given in angstroms and the superscripts indicate the spin multiplicity. The arrows indicate the spin polarization at the Co atoms. AF stands for antiferromagnetic coupling.

clusters are calculated to contain two molecular O_2 units. In the neutral cluster, however, the oxygen−oxygen bond of the O_2 units is more elongated than in the cation. The anionic CoO_4^- cluster contains both atomically and molecularly bound oxygen with the oxygen−oxygen bond of the O_2 unit elongated to a length of 1.41 Å. The experimental fragmentation studies again confirm that the CoO_4^+ cluster loses molecular O_2. CoO_4^+ also loses atomic oxygen suggesting that the O−O bond of the remaining O_2 unit is broken in subsequent collisions. Indeed, the O−O bond length in CoO_2^+ is calculated to be elongated to 1.32 Å. Therefore, after O_2 is lost from CoO_4^+, the remaining O_2 unit is collisionally dissociated resulting in the loss of atomic oxygen. Unfortunately, we were unable to produce sufficient intensity of the CoO_4^- anion to study its fragmentation experimentally.

The ground state geometries for neutral, cationic and anionic Co_2O_y ($y = 1-6$) clusters are shown in Figure 5. A central structure formed of a Co_2O_2 ring with oxygen atoms bridging each Co atom was found in this series, in analogy to Fe_2O_y clusters.[2,3] At higher oxygen content, attachment to the cobalt atoms outside of the ring was found, with molecular O_2 units present for clusters with four and more oxygen atoms. Three Co−O bond lengths were characteristic in these clusters. A bond length in the range 1.72−1.84 Å within the ring, a shorter bond length around 1.60 Å for oxygen bonded atomically outside of the ring and, a larger bond from the Co atoms to the molecular O_2 units on the order of 1.81−1.89 Å. In general, high spin states were found for the ground states of the neutral and charged Co_2O_y clusters, as shown in Figure 5. An antiferromagnetic coupling between the Co sites leading to a low spin state,

TABLE 4: Calculated Dissociation Energies of Atomic DE(O), and Molecular Oxygen DE(O_2) from Anionic, Neutral and Cationic Co_2O_y ($y = 1-6$) Clusters Corresponding to the Graphs in Figure 6[a]

	DE(O)	DE(O_2)	EA	IP
$^5Co_2$			0.72	7.16
$^5Co_2O$	5.61		0.9	7.49
$^1Co_2O_2$ (AF)	5.59	5.03	1.76	7.9
$^5Co_2O_3$	4.74	4.15	2.75	9.05
$^5Co_2O_4$	4.59	3.15	3.85	9.8
$^1Co_2O_5$ (AF)	3.74	2.15	3.52	9.76
$^7Co_2O_6$	3.20	0.76	3.78	9.32
$^6Co_2O^+$	5.28			
$^6Co_2O_2^+$	5.18	4.28		
$^6Co_2O_3^+$	3.59	2.59		
$^6Co_2O_4^+$	3.84	1.26		
$^2Co_2O_5^+$ (AF)	3.78	1.45		
$^8Co_2O_6^+$	3.64	1.24		
$^6Co_2O^-$	5.80			
$^2Co_2O_2^-$ (AF)	6.45	6.07		
$^6Co_2O_3^-$	5.73	6.0		
$^4Co_2O_4^-$	5.69	5.24		
$^4Co_2O_5^-$	3.40	2.92		
$^6Co_2O_6^-$	3.46	0.69		

[a] AF stands for antiferromagnetic coupling of Co sites. Electron affinities (EA) and ionization potentials (IP) of neutral Co_2O_y ($y = 0-6$) clusters. All values are given in units of eV.

however, was found for Co_2O_5, $Co_2O_5^+$ and $Co_2O_2^-$. Although, for these clusters, low lying energy states with a ferromagnetic coupling and a high spin state were found only 0.04 to 0.09 eV higher in energy. Similarly, though for $Co_2O_3^+$ a sextet ground state was found, an antiferromagnetic state in a doublet spin state was located 0.012 eV higher in energy.

Ionic charge state was found to influence the structures of the clusters containing two cobalt atoms. For the neutral and anionic clusters, all of the oxygen binds atomically up to a saturation of four oxygen atoms. The fifth and sixth oxygen atoms form molecular O_2 units outside of the Co_2O_2 ring. An interesting variation is that the anionic $Co_2O_3^-$ cluster binds oxygen atomically to one cobalt atom rather than in a bridging fashion. In contrast, in the case of cationic clusters, molecular O_2 units become present at a saturation of four oxygen atoms. In general, the cobalt−cobalt bonds are longer in the cations than in the neutral and anionic clusters. The experimental fragmentation data confirm the loss of atomic oxygen from $Co_2O_2^+$ and the fragmentation of CoO from the $Co_2O_3^-$ anion indicating that the oxygen is atomically bound and that the cobalt−cobalt bond is fairly weak, respectively. For the oxygen rich clusters, Co_2O_5 and Co_2O_6, it is clear that the O−O bond in the molecular O_2 units is more elongated in the anionic and neutral clusters than in the cationic species. The experimental fragmentation studies indicate the loss of one O_2 unit from the anionic $Co_2O_5^-$ cluster and two molecular O_2 units from cationic $Co_2O_6^+$ verifying the theoretically calculated structures.

One factor that determines whether the oxidation of CO is favorable by a given metal oxide cluster is the oxygen dissociation energy. To determine whether the anionic clusters which exhibit enhanced oxidation reactivity contain particularly weakly bound oxygen atoms, the oxygen dissociation energies were calculated. The energy required to remove both atomic and molecular oxygen from cobalt oxide clusters containing one and two cobalt atoms is displayed in Tables 3 and 4, as well as the ionization potential (IP) and electron affinity (EA) of the neutral clusters. The oxygen dissociation energies are also plotted in Figure 6. The atomic oxygen dissociation energy for

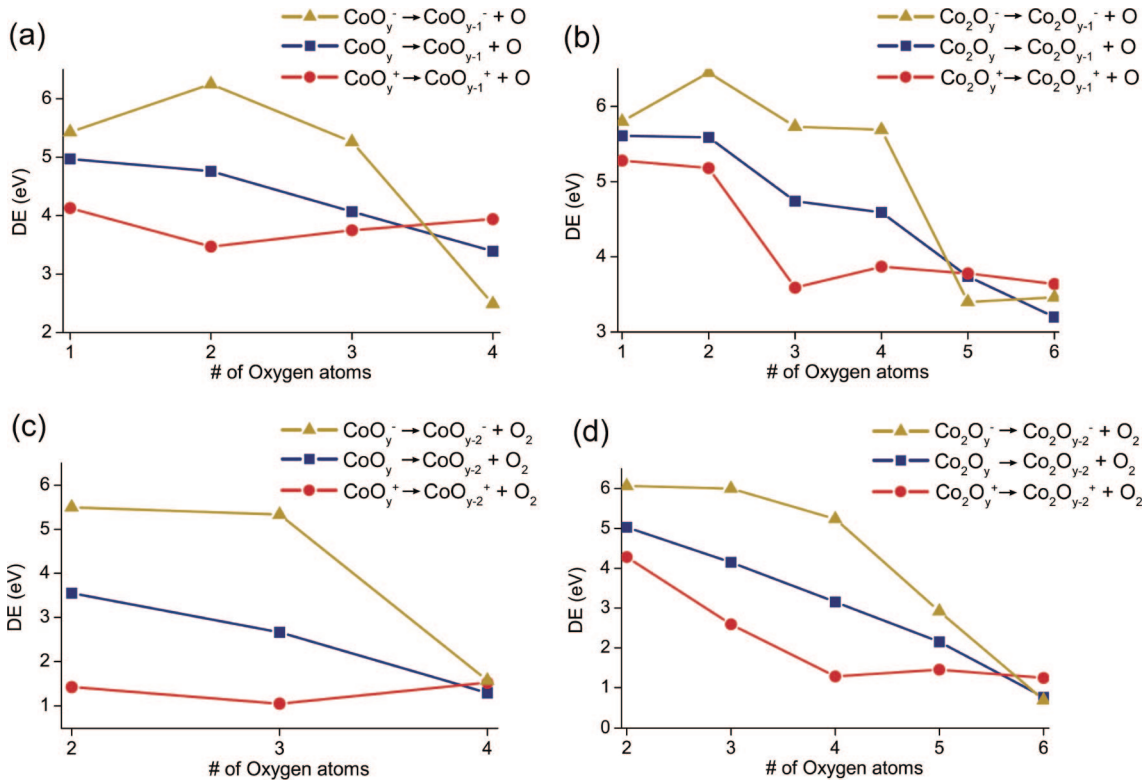

Figure 6. Plots of the calculated dissociation energy (DE) associated with removing an O atom from (a) CoO_y ($y = 1-4$) clusters, (b) Co_2O_y ($y = 1-6$) clusters, and removing an O_2 subunit from (c) CoO_y ($y = 1-4$) clusters and (d) Co_2O_y ($y = 1-6$) clusters.

anionic oxide clusters containing one cobalt atom is shown to increase initially with the addition of oxygen and then to decrease sharply at higher oxygen coverage. The neutral clusters exhibit a steady decrease in atomic oxygen dissociation energy with higher oxygen saturation. The atomic oxygen dissociation energies for the cationic clusters, in contrast, decrease initially and then increase steadily with the addition of more oxygen. This is because at higher oxygen content, the oxygen binds molecularly to cationic cobalt clusters. Therefore, the O−O bond becomes less activated with increasing oxygen coverage and it takes more energy to dissociate it and release a single O atom.

For neutral and cationic cobalt oxides containing two cobalt atoms, the atomic oxygen dissociation energies are shown to decrease substantially at oxygen coverage greater than two atoms. The anionic clusters, in contrast, exhibit a sharp increase in dissociation energy at a coverage of two oxygen atoms and then a plateau at three and four oxygen atoms, followed by a decrease at higher saturation. The sharp decrease in oxygen dissociation energy at $Co_2O_3^-$ and $Co_2O_5^-$ correlates well with the enhanced oxidation reactivity observed experimentally for the $Co_2O_3^-$ and $Co_2O_5^-$ clusters. Figure 6 also indicates that the atomic oxygen dissociation energy for the anionic clusters is larger than for the neutral and cationic species up to a saturation of three oxygen atoms for the one cobalt atom clusters and four oxygen atoms for the two cobalt atom clusters.

The molecular O_2 dissociation energies are also displayed in Figure 6. For both the one and two cobalt atom clusters the dissociation energies decline with increasing oxygen coverage. The charge state is found to exert a pronounced influence on the dissociation energy of molecular O_2. For the one and two cobalt atom clusters, the anionic species have much larger dissociation energies than the neutral and cationic clusters. At coverage of four oxygen atoms, however, the dissociation energies of the three different charge states converge to a value of around 1.5 eV for the one cobalt atom clusters, whereas for the clusters with two cobalt atoms the dissociation energy converges to around 1.1 eV at a saturation of six oxygens.

TABLE 5: Calculated Energies for the Reaction of Anionic and Cationic CoO_y ($y = 0-3$) Clusters with CO, Corresponding to the Attachment of CO to the CoO_y Clusters

			ΔE (eV)
$^3Co^- + {}^1CO$	→	$^3CoCO^-$	−2.07
$^5CoO^- + {}^1CO$	→	$^5OCCoO^-$	−1.34
$^1CoO_2^- + {}^1CO$	→	$^1OCCoO_2^-$	−1.24
$^3CoO_3^- + {}^1CO$	→	$^3OCCoO_3^-$	−0.13
$^3Co^+ + {}^1CO$	→	$^3CoCO^+$	−2.38
$^5CoO^+ + {}^1CO$	→	$^5OCCoO^+$	−1.71
$^3CoO_2^+ + {}^1CO$	→	$^3OCCoO_2^+$	−2.27
$^3CoO_3^+ + {}^1CO$	→	$^3OCCoO_3^+$	−1.33

Another factor that determines whether the oxidation of CO is favorable by a given cluster is its binding energy to that species. To gain insight into how stoichiometry and ionic charge state influence the binding of CO to cobalt oxide clusters, the CO binding energies and ground state geometries were calculated for the example species $CoCO^{\pm}$, $CoOCO^{\pm}$, $CoO_2CO^{\pm}$ and $CoO_3CO^{\pm}$. The CO binding energies of minima corresponding to CO attachment, and those of the ground state geometries are provided respectively in Tables 5 and 6 for each cluster, in both possible charge states. Inspection of Tables 5 and 6 reveals that the CO binding energies are consistently larger for the cationic cobalt oxides than for the anionic clusters. Furthermore, with increasing oxygen content there are substantial variations in the CO binding energy. Examination of the calculated ground state geometries presented in Figure 7 shows that the most stable configurations generally contain CO_2 units. For the cationic clusters, although CO binds initially to the positively charged cobalt atom, the energy gained through the formation of the O−CO bond makes the structures with the CO_2 subunits the

TABLE 6: Calculated Energies for the Reaction of Anionic and Cationic CoO_y ($y = 0-3$) Clusters with CO, Corresponding to the Ground State Structures Shown in Figure 7

			ΔE (eV)
$^3Co^- + {}^1CO$	→	$^3CoCO^-$	−2.07
$^5CoO^- + {}^1CO$	→	$^3CoOCO^-$	−2.83
$^1CoO_2^- + {}^1CO$	→	$^3CoO_2CO^-$	−2.50
$^3CoO_3^- + {}^1CO$	→	$^3CoO_3CO^-$	−1.77
$^3Co^+ + {}^1CO$	→	$^3CoCO^+$	−2.38
$^5CoO^+ + {}^1CO$	→	$^3CoOCO^+$	−3.35
$^3CoO_2^+ + {}^1CO$	→	$^5CoO_2CO^+$	−4.25
$^3CoO_3^+ + {}^1CO$	→	$^3CoO_3CO^+$	−3.99

lowest energy configurations. The anionic clusters also contain CO_2 subunits with the exception of $CoOCO^-$. One interesting structural variation between the cationic and anionic clusters is that the cations bind CO exclusively as a linear OCO subunit. The anionic clusters, in contrast, bind CO_2 in a bent ring configuration containing both Co−C and Co−O bonds.

To obtain insight into the energetics of CO oxidation in the presence of anionic cobalt oxide clusters, an example energy profile for the oxidation of CO by $Co_2O_3^-$ was calculated and is presented in Figure 8a. The adsorption of CO onto the $Co_2O_3^-$ cluster followed by the formation of a CO_2 unit results in a complex which is more stable than the reactants by 2.22 eV. Loss of CO_2 then requires 1.79 eV and results in a $Co_2O_2^-$ product that is lower in energy than the reactants by 0.43 eV. The initial product configuration then rearranges to the global minimum structure of $Co_2O_2^-$ which is 0.61 eV more stable than the reactants. Consequently, the oxidation of CO by $Co_2O_3^-$ is overall exothermic and involves an easily surmountable step.

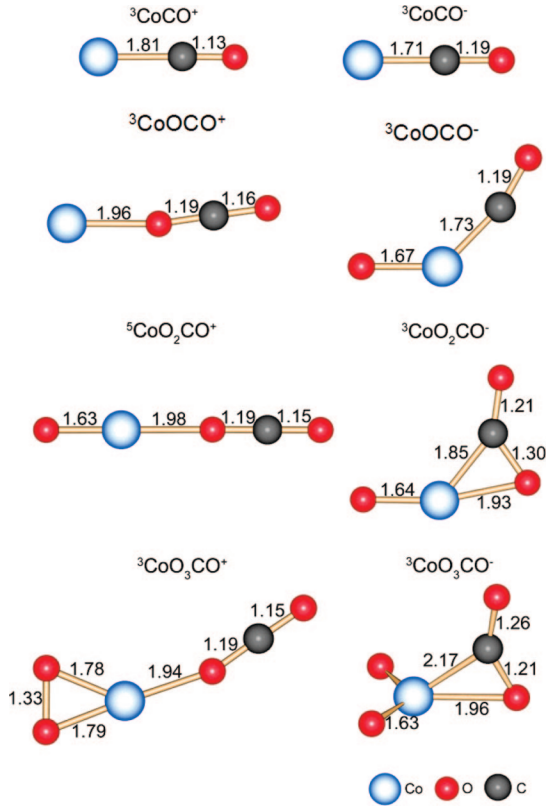

Figure 7. Calculated ground state geometries of cationic and anionic CoO_yCO ($y = 0-3$) clusters. The bond lengths are given in angstroms and the superscripts indicate the spin multiplicity.

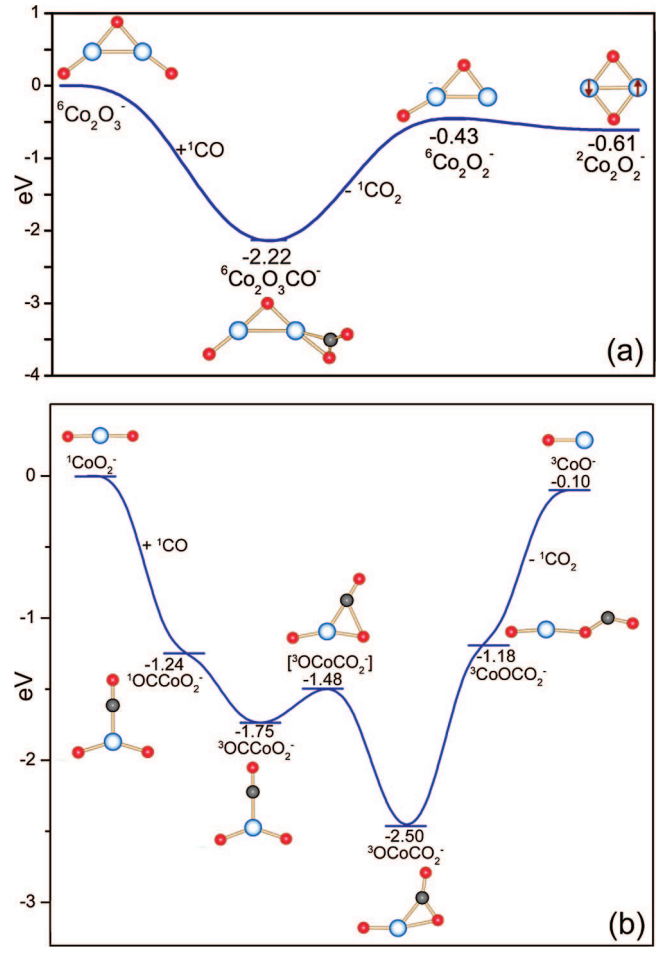

Figure 8. Plot of the calculated change in energy (ΔE) for each step of the reaction pathway of (a) $Co_2O_3^-$ and (b) CoO_2^- with CO. The superscripts indicate spin multiplicity.

To facilitate a comparison between the anionic cobalt oxides that were found to be particularly reactive for CO oxidation and those that were not, the reaction profile for the oxidation of CO by CoO_2^- was calculated and is shown in Figure 8b. Adsorption of CO onto CoO_2^- results in a complex which is 1.24 eV more stable than the reactants. A change in spin multiplicity from singlet to triplet further stabilizes the cluster. Formation of a CO_2 unit involves a small barrier and creates a complex that is 2.50 eV lower in energy than the reactants. Dissociation of CO_2 forms the final CoO^- product which is only 0.10 eV more stable than the reactants. Therefore, the oxidation of CO by CoO_2^- is calculated to be much less exothermic than $Co_2O_3^-$. Correspondingly, only a very minor atomic oxygen loss product is observed experimentally.

An example energy profile was calculated for the adsorption of CO accompanied by the loss of O_2 on cationic cobalt oxide clusters. Figure 9 shows that the adsorption of CO onto CoO_2^+ results in a complex that is 2.27 eV more stable than the reactants (a much larger energy gain, compared to only 1.24 eV for the CO attachment to CoO_2^-, as shown in Table 5). This initial complex rearranges through dissociation of one Co−O bond forming a complex with a Co−O−O structure that is, after a change of multiplicity from triplet to quintet, 1.92 eV lower in energy than the reactants. Dissociation of molecular O_2 forms the $CoCO^+$ product, which is 0.96 eV more stable than the reactants. Therefore, the overall process for the adsorption of CO accompanied by the loss of O_2 is exothermic. The energy profile for the formation of the minor product Co^+

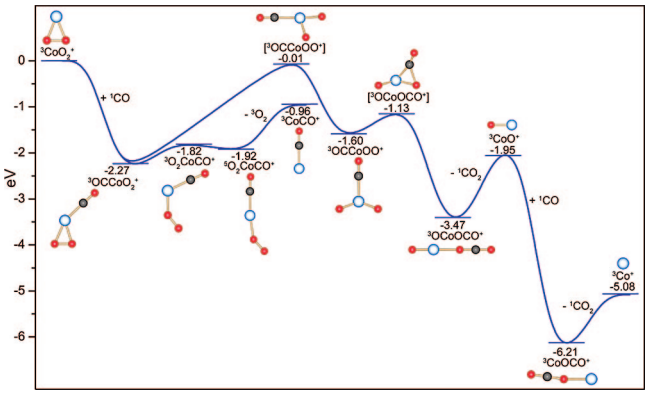

Figure 9. Plot of the calculated change in energy (ΔE) for each step of the reaction pathway of CoO_2^+ with CO. The superscripts indicate spin multiplicity.

was also calculated. This mechanism assumes that the cluster oxidizes CO, which requires breaking the O−O bond of the molecular O_2 unit. Due to the large amount of energy required for this process the reaction must proceed through a state that is only 0.01 eV lower in energy than the reactants. Subsequent formation of a CO_2 unit is highly exothermic, resulting in a complex that is 3.47 eV more stable than the reactants. Dissociation of CO_2 forms a CoO^+ intermediate that is 1.95 eV lower in energy than the reactants. Finally, oxidation of an additional CO molecule produces the Co^+ product in a process that is exothermic overall by 5.08 eV. Despite the highly exothermic nature of this process, because it proceeds through a step that is almost equivalent to the energy of the reactants, it is less favorable than the reaction where O_2 is replaced by CO. These theoretical findings are supported by the experimental data shown in Figure 3 which show that the $CoCO^+$ product is far more intense than the Co^+ product.

Implications for Catalysis. Our results concerning the oxygen dissociation and carbon monoxide binding energy for cobalt clusters suggest that active sites with both partial positive and negative charge states may play a role in the oxidation of CO. Clearly, for cationic clusters, oxygen binds preferentially in the molecular form with little elongation of the oxygen−oxygen bond as shown in Figures 4 and 5. These O_2 units are so weakly bound, in fact, that they are easily fragmented through collision with an inert gas or through the exothermic adsorption of CO onto the cluster. Therefore, it is unlikely that cationic clusters containing molecularly bound oxygen would be active for the oxidation of CO. Anionic clusters, in contrast, bind oxygen mainly in the atomic form where activation of the strong oxygen−oxygen double bond has already occurred. Interestingly, oxygen binds more strongly in both the atomic and molecular form to negatively charged metal centers. An analogy to the terminology of bulk-phase catalysis may be useful here. Typically, there is an optimum binding energy of reactant molecules to catalyst particles that results in the highest catalytic activity. The reactant molecules must bind strongly enough to the catalyst to become activated but not so strongly as to poison the surface.[52,53] Therefore, despite the fact that oxygen binds more strongly in negatively charged cobalt oxide clusters, it is highly activated or bound in the atomic form where activation is complete. Consequently, it is more favorable for CO oxidation to occur in the presence of negatively charged cobalt oxides. Positively charged sites, in contrast, serve as efficient acceptors of the lone pair of electrons of CO enabling strong binding of this molecule, as evidenced by the experimentally observed CO attached complex clusters ($Co_xO_yCO^+$), and by our calculations of CO binding energies. A DFT study of Co_2Co clusters by Tremblay et al.[54] additionally supports this argument. Although the carbon atom of CO binds to one cobalt atom in anionic Co_2CO^-, in the cationic cluster Co_2CO^+ the carbon atom binds both cobalt atoms in a bridge configuration. Therefore, it is likely that in the bulk phase, sites with a partial positive charge will bind large quantities of CO which will, subsequently, migrate to a neighboring partially negatively charged site where oxidation will occur.

The findings presented herein demonstrate that oxide clusters of different 3d transition metals have specific stoichiometries that are most active for the oxidation of CO. Cobalt, in comparison to iron, has an electronic configuration with one more d electron in its valence shell (Co:$4s^2d^7$, Fe:$4s^2d^6$), leading to a different common bulk-phase stoichiometry (Co:Co_3O_4, Fe:Fe_2O_3). For anionic iron oxide clusters we demonstrated, in a previous publication,[2] that species with one more oxygen atom than iron atom (FeO_2^- and $Fe_2O_3^-$), are the most active toward CO oxidation. In the present study, anionic cobalt oxides having the same or higher oxygen saturation ($Co_2O_3^-$, $Co_2O_5^-$, $Co_3O_5^-$ and $Co_3O_6^-$) were identified to be most selective toward CO_2 formation. In general, the calculated oxygen atom dissociation energies for anionic cobalt oxide clusters containing one cobalt atom are similar to those of iron oxides. However, for the anionic two cobalt atom clusters, the oxygen dissociation energies are generally lower than for iron oxides. This may partially explain the more frequent observation of collisional O, O_2 and CoO_y loss observed with anionic cobalt oxides compared to iron oxides.

In another previous publication[3] we showed that cationic iron oxide clusters containing three or fewer oxygen atoms are the most selective for CO oxidation whereas clusters with higher oxygen content favor the adsorption of CO. For cationic cobalt oxides, in contrast, we were unable to experimentally identify any clusters with enhanced activity for CO oxidation. Instead, the dominant reaction channel was the adsorption of CO accompanied by the loss of molecular O_2. The calculated atomic oxygen dissociation energies of cationic cobalt oxide clusters containing one and two cobalt atoms are, in general, slightly lower than for iron oxides. Furthermore the molecular O_2 dissociation energies are also calculated to be generally lower for cobalt than for iron. As mentioned above, as the strength of O_2 binding correlates well with the degree of activation of the O−O bond, this likely explains why iron oxide cation clusters, which contain more strongly bound, and therefore, activated O_2 units, oxidize CO but cobalt oxide cations do not.

Conclusion

Through a combination of gas-phase experiments and density functional theory calculations we have provided molecular level insight into the influence of ionic charge state and stoichiometry on the structure of cobalt oxide clusters and their reactivity with CO. Anionic cobalt oxides with the stoichiometries $Co_2O_3^-$, $Co_2O_5^-$, $Co_3O_5^-$ and $Co_3O_6^-$ were found to be particularly active toward the transfer of a single oxygen atom to CO forming CO_2. The enhanced reactivity of these anionic clusters is attributed, on the basis of theory, to their relatively low atomic oxygen dissociation energy, which makes CO oxidation energetically favorable. Cationic cobalt oxides, in contrast, are shown to react preferentially through the adsorption of CO onto the cluster accompanied by the loss of molecular O_2 units. Calculations establish that this O_2 replacement reaction is favored by the weak binding of molecular O_2 and the strong binding of CO to positively charged cobalt centers. Our results suggest

that a combination of active sites, some positively charged and others negatively charged, are necessary to enable the efficient oxidation of CO to CO_2 in the presence of cobalt oxides.

Acknowledgment. G.E.J., N.M.R., E.C.T. and A.W.C. gratefully acknowledge the U.S. Department of Energy, Grant No. DE-FG02-92ER14258, for financial support of the experimental work reported herein. JUR and SNK acknowledge support from U.S. Department of Energy Grant DE-FG02-96ER45579. Part of the deMon2k calculations were performed on the computational equipment of DGSCA UNAM, particularly at the super computer KanBalam.

Note Added after ASAP Publication. This article posted ASAP on October 15, 2008. Equation 10 has been revised. The correct version posted on October 21, 2008.

References and Notes

(1) (a) Castleman, A. W., Jr.; Bowen, K. H., Jr. *J. Phys. Chem.* **1996**, *100*, 12911. (b) Castleman, A. W., Jr.; Khanna, S. N.; Sen, A.; Reber, A. C.; Qian, M.; Davis, K. M.; Peppernick, S. J.; Ugrinov, A.; Merritt, M. D. *Nano Letters* **2007**, *7*, 2734.

(2) Reilly, N. M.; Reveles, J. U.; Johnson, G. E.; Castleman, A. W., Jr.; Khanna, S. N. *J. Phys. Chem. A* **2007**, *111*, 4158.

(3) Reilly, N. M.; Reveles, J. U.; Johnson, G. E.; del Campo, J. M.; Khanna, S. N.; Köster, A. M.; Castleman, A. W., Jr. *J. Phys. Chem. C* **2007**, *111*, 19086.

(4) Reilly, N. M.; Reveles, J. U.; Johnson, G. E.; Castleman, A. W., Jr.; Khanna, S. N. *Chem. Phys. Lett.* **2007**, *435*, 295.

(5) Wang, Y. Z.; Zhao, Y. X.; Gao, C. G.; Liu, D. S. *Catal. Lett.* **2007**, *116*, 136.

(6) Lopes, I.; Davidson, A.; Thomas, C. *Catal. Commun.* **2007**, *8*, 2105.

(7) Solsona, B.; Vazquez, I.; Garcia, T.; Davies, T. E.; Taylor, S. H. *Catal. Lett.* **2007**, *116*, 116.

(8) Davies, T. E.; Garcia, T.; Solsona, B.; Taylor, S. H. *Chem. Commun.* **2006**, *32*, 3417–3419.

(9) Böhme, D. K.; Schwarz, H. *Angew. Chem., Int. Ed.* **2005**, *44*, 2336.

(10) Kim, Y. D. *Int. J. Mass. Spectrom.* **2004**, *238*, 17.

(11) Pramann, A.; Koyasu, K.; Nakajima, A.; Kaya, K. *J. Phys Chem. A* **2002**, *106*, 4891.

(12) Uzonova, E.; St Nikolov, G.; Mikosch, H. *J. Phys. Chem. A* **2002**, *106*, 4104.

(13) Yoon, B.; Hakkinen, H.; Landman, U.; Worz, A. S.; Antonietti, J. M.; Abbet, S.; Judai, K.; Heiz, U. *Science* **2005**, *307*, 403.

(14) Liu, F. Y.; Li, F. X.; Armentrout, P. B. *J. Chem. Phys.* **2005**, *123*, 064304.

(15) Andersson, M.; Persson, J. L.; Rosen, A. *J. Phys. Chem.* **1996**, *100*, 12222.

(16) Kapiloff, E.; Ervin, K. M. *J. Phys. Chem. A* **1997**, *101*, 8460.

(17) Bell, R. C.; Zemski, K. A.; Justes, D. R.; Castleman, A. W., Jr. *J. Chem. Phys.* **2001**, *114*, 798.

(18) Köster, A. M.; Calaminici, P.; Casida, M. E.; Flores-Moreno, R.; Geudtner, G.; Goursot, A.; Heine, T.; Ipatov, A.; Janetzko, F.; M. del Campo, J.; Patchkovskii, S.; Reveles, J. U.; Salahub, D. R.; Vela, A. deMon2k, ver 2.4; The International deMon Developers Community: Cinvestav, México, 2007;available at http://www.deMon-software.com.

(19) (a) Perdew, J. P.; Wang, Y. *Phys. Rev. B* **1986**, *33*, 8800. (b) Perdew, J. P. *Phys. Rev. B* **1986**, *33*, 8822; (c) **1986**, *34*, 7406.

(20) Calaminici, P.; Janetzko, F.; Köster, A. M.; Mejia-Olivera, R.; Zuniga-Gutierrez, B. *J. Chem. Phys.* **2007**, *126*, 044108.

(21) Pederson, M. R.; Jackson, K. A. *Phys. Rev. B* **1990**, *41*, 7453.

(22) Jackson, K.; Pederson, M. R. *Phys. Rev. B* **1990**, *42*, 3276.

(23) Porezag, D.; Pederson, M. R. *Phys. Rev. A* **1999**, *60*, 2840.

(24) Perdew, J. P. In *Electronic Structure of Solids*; Ziesche, P., Eschrig, H., Eds.; Akademie Verlag: Berlin, 1991.

(25) Weisshaar, J. C. *J. Chem. Phys.* **1988**, *90*, 1429.

(26) Kant, A.; Strauss, B. *J. Chem. Phys.* **1964**, *41*, 3806.

(27) Jamorski, C.; Martínez, A.; Castro, M.; Salahub, D. R. *Phys. Rev. B* **1997**, *55*, 10905.

(28) Yanagisawa, S.; Tsuneda, T.; Hirao, K. *J. Chem. Phys.* **2000**, *112*, 545.

(29) Gutsev, G. L.; Khanna, S. N.; Jena, P. *Chem. Phys. Lett.* **2001**, *345*, 481.

(30) Gutsev, G. L.; Bauschlicher, C. W., Jr. *J. Phys. Chem. A* **2003**, *107*, 4755.

(31) Datta, S.; Kabir, M.; Ganguly, S.; Sanyal, B.; Saha-Dasgupta, T.; Mookerjee, A. *Phys. Rev. B* **2007**, *76*, 014429.

(32) Shim, I.; Gingerich, K. A. *J. Chem. Phys.* **1983**, *78*, 5693.

(33) Barden, C. J.; Rienstra-Kiracofe, J. C.; Schaefer, H. F., III *J. Chem. Phys.* **2000**, *113*, 690.

(34) Keller, E. *Chem. Z.* **1980**, *14*, 56, http://www.krist.uni-freiburg.de/ki/Mitarbeiter/Keller/schakal.html

(35) *CRC Handbook of Chemistry and Physics*, 67th ed.; Weast, R. C., Ed.; CRC Press, Inc.: Boca Raton, FL, 1986.

(36) *Comprehensive Handbook of Chemical Bond Energies*; Luo, Y. -R., Eds.;CRC Press: Boca Raton, FL, 2007.

(37) Chase, M. W.; Davies, C. A.; Downey, J. R.; Frurip, D. J.; McDonald, R. A.; Syverud, A. N. JANAF Thermochemical Tables, 3rd ed. *J. Phys. Chem Ref. Data* **1985**, (Suppl. 1), 14.

(38) Callomon, J. H.; Hirota, E.; Kuchitsu, K.; Lafferty, W. J.; Maki, A. G.; Pote, C. S. *Structure Data of Free Polyatomic Molecules*; Hellwege, K. H., Hellwege, A. M., Eds.; Landolt-Boernstein New Series, Group II, Vol. 7: Springer-Verlag: Berlin, 1976.

(39) Lias, S. G.; Bartmess, J. E.; Leibman, J. F.; Levin, J. L.; Levin, R. D.; Mallard, W. G. *J. Phys. Chem. Ref. Data* **1988**, 17 Suppl. No. 1.

(40) Hales, D. A.; Su, C. X.; Lian, L.; Armentrout, P. B. *J. Chem. Phys.* **1994**, *100*, 1049.

(41) Russon, L. M.; Heidecke, S. A.; Birke, M. K.; Conceicao, J. J.; Armentrout, P. B.; Morse, M. D. *Chem. Phys. Lett.* **1993**, *204*, 235.

(42) (a) Fisher, E. R.; Elkind, J. L.; Clemmer, D. E.; Georgiadis, R.; Loh, S. K.; Aristov, N.; Sunderlin, L. S.; Armentrout, P. B. *J. Chem. Phys.* **1990**, *93*, 2676. (b) Fisher, E. R.; Armentrout, P. B. *J. Phys. Chem.* **1990**, *94*, 1674. (c) Armentrout, P. B.; Kickel, B. L. In *Organometallic Ion Chemistry*; Freiser, B. S., Ed.; Kluwer: Dordrecht, The Netherlands, 1996, pp 1−45.

(43) (a) Drzaic, P. S.; Marks, J.; Brauman, J. I. *Gas Phase Ion Chemistry*; Bowers, M. T., Ed.; Academic Press: Orlando, 1984; Vol. 3, Chapter 21, p 167. (b) Mead, R. D.; Stevens, A. E.; Lineberg, W. C. *Gas Phase Ion Chemistry*; Bowers, M. T., Eds.; Academic Press: Orlando, 1984; Chapter 21, p 167, Vol. 3, Chapter 22, p 213.

(44) Page, R. H.; Gudeman, C. S. *J. Opt. Soc. Am. B* **1990**, *7*, 1761.

(45) Calculated from $IP(CoO) = D_o(Co-O) + IP(Co) - D_o(Co^+-O)$ in ref 14.

(46) Li, S.; Wang, L. S. *J. Chem. Phys.* **1999**, *111*, 8389.

(47) Cited in: (a) Gustev, G. L.; Rao, B. K.; Jena, P. *J. Phys. Chem. A* **2000**, *104*, 11961.

(48) Kurth, S.; Perdew, J. P.; Blaha, P. *Int. J. Quantum Chem.* **1999**, *75*, 889.

(49) M. J. Frisch, M. J.; Trucks, G. W.; Schlegel, H. B.; Scuseria, G. E.; Robb, M. A.; Cheeseman, J. R.; Montgomery, J. A. Jr.; Vreven, T.; Kudin, K. N.; Burant, J. C.; Millam, J. M.; Iyengar, S. S.; Tomasi, J.; Barone, V.; Mennucci, B.; Cossi, M.; Scalmani, G.; Rega, N.; Petersson, G. A.; Nakatsuji, H.; Hada, H.; Ehara, M.; Toyota, K.; Fukuda, R.; Hasegawa, J.; Ishida, M.; Nakajima, T.; Honda, Y.; Kitao, O.; Nakai, H.; Klene, M.; Li, X.; Knox, J. E.; Hratchian, H. P.; Cross, J. B.; Bakken, V.; Adamo, C.; Jaramillo, J.; Gomperts, R.; Stratmann, R. E.; Yazyev, O.; Austin, A. J.; Cammi, R.; Pomelli, C.; Ochterski, J. W.; Ayala, P. Y.; Morokuma, K.; Voth, G. A.; Salvador, P.; Dannenberg, J. J.; Zakrzewski, V. G.; Dapprich, S.; Daniels, A. D.; Strain, M. C.; Farkas, O.; Malick, D. K.; Rabuck, A. D.; Raghavachari, K.; Foresman, J. B.; Ortiz, J. V.; Cui, Q.; Baboul, A. G.; Clifford, S.; Cioslowski, J.; Stefanov, B. B.; Liu, G.; Liashenko, A.; Piskorz, P.; Komaromi, I.; Martin, R. L.; Fox, D. J.; Keith, T.; Al-Laham, M. A.; Peng, C. Y.; Nanayakkara, A.; Challacombe, M.; Gill, P. M. W.; Johnson, B.; Chen, W.; Wong, M. W.; Gonzalez, C.; Pople, J. A. *Gaussian 03*, revision D.02; Gaussian, Inc.: Wallingford, CT, 2004.

(50) Perdew, J. P.; Burke, K.; Ernzerhof, M. *Phys. Rev. Lett.* **1996**, *77*, 3865.

(51) Becke, A. D. *J. Chem. Phys.* **1993**, *98*, 5648.

(52) Van Santen, R. A.; Neurock, M. *Molecular Heterogeneous Catalysis*; Wiley-VCH: Weinheim, 2006.

(53) Somorjai, G. A. *Introduction to Surface Chemistry and Catalysis*; John Wiley and Sons Inc.: New York, 1994.

(54) Tremblay, B.; Manceron, L.; Gutsev, G. L.; rews, L.; Partridge, H., II *J. Chem. Phys.* **2002**, *117*, 8479.

JP805186R